

# Shape sensitivity analysis in mixed-mode fracture mechanics

G. Chen, S. Rahman, Y. H. Park

282

**Abstract** This paper presents a new method for continuum-based shape sensitivity analysis for a crack in a homogeneous, isotropic, and linear-elastic body subject to mixed-mode (modes I and II) loading conditions. The method is based on the material derivative concept of continuum mechanics, domain integral representation of an interaction integral, and direct differentiation. Unlike virtual crack extension techniques, no mesh perturbation is needed in the proposed method to calculate the sensitivity of stress-intensity factors. Since the governing variational equation is differentiated prior to the process of discretization, the resulting sensitivity equations are independent of approximate numerical techniques, such as the finite element method, boundary element method, meshless methods, or others. In addition, since the interaction integral is represented by domain integration, only the first-order sensitivity of the displacement field is needed. Two numerical examples are presented to illustrate the proposed method. The results show that the maximum difference in the sensitivity of stress-intensity factors calculated using the proposed method and reference solutions obtained by analytical or finite-difference methods is less than four percent.

## 1

### Introduction

Sensitivity analysis of a crack-driving force plays an important role in many fracture-mechanics applications involving the stability and arrest of crack propagation, reliability analysis, parameter identification, or other considerations. For example, the derivatives of the stress-intensity factor (SIF) or other fracture parameters are of-

ten required to predict the probability of fracture initiation and/or instability in cracked structures. The first- and second-order reliability methods [1], frequently used in probabilistic fracture mechanics [2–8], require the gradient and Hessian of the performance function with respect to random parameters. In linear-elastic fracture mechanics (LEFM), the performance function is built on SIF. Hence, both first- and/or second-order derivatives of SIF are needed for probabilistic analysis. The calculation of these derivatives with respect to load and material parameters, which constitutes size-sensitivity analysis, is not unduly difficult. However, the evaluation of response derivatives with respect to crack size is a challenging task, since it requires shape sensitivity analysis. Using a brute-force type finite-difference method to calculate the shape sensitivities is often computationally expensive, in that numerous repetitions of deterministic finite element analysis may be required for a complete reliability analysis. Furthermore, if the finite-difference perturbations are too large relative to finite element meshes, the approximations can be inaccurate, whereas if the perturbations are too small, numerical truncation errors may become significant. Therefore, an important requirement of some fracture-mechanics applications is to evaluate the rates of SIF accurately and efficiently.

Some methods have already appeared to predict the sensitivities of SIF under mode-I condition. In 1988, Lin and Abel [9] introduced a direct-integration approach for a virtual crack extension technique that employs the variational formulation and a finite element method (FEM) to calculate the first derivative of SIF for a structure containing a single crack. This method maintains all of the advantages of similar virtual crack extension techniques introduced by deLorenzi [10, 11], Haber and Koh [12], and Barbero and Reddy [13], but adds a capability to calculate the derivatives of the SIF. Subsequently, Hwang et al. [14] generalized this method to calculate both first- and second-order derivatives for structures involving multiple crack systems, axisymmetric stress state, and crack-face and thermal loading. A salient feature of this method is that SIFs and their derivatives can be evaluated in a single analysis. However, this method requires mesh perturbation – a fundamental requirement of all virtual crack extension techniques. For second-order derivatives, the number of elements affected by mesh perturbation surrounding the crack tip has a significant effect on solution accuracy [14]. Recently, Feijóo et al. [15] applied the concepts of shape sensitivity analysis [16] to calculate the first-order derivative of the potential energy. Since the energy release rate

Received 19 September 2000

G. Chen, S. Rahman (✉)  
Department of Mechanical Engineering,  
The University of Iowa,  
Iowa City, IA 52242  
e-mail: rahman@engineering.uiowa.edu

Y. H. Park  
Department of Mechanical Engineering,  
New Mexico State University,  
Las Cruces, NM 88003

This effort was supported by the U.S. National Science Foundation (NSF) Faculty Early Career Development Award (Grant No. CMS-9733058) to S. Rahman. The NSF program directors were Drs. Sunil Saigal and Ken Chong.

(ERR) is the first-order derivative of potential energy, the ERR or SIF can be calculated using this approach, without any mesh perturbation. Later, Taroco [17] extended this approach to formulate the second-order sensitivity of potential energy to predict the first-order derivative of the ERR. In practice, however, this presents a formidable task, since it involves calculation of second-order stress and strain sensitivities. To overcome this difficulty, Chen et al. [18, 19] invoked the domain integral representation of the  $J$ -integral and used the material derivative concept of continuum mechanics to obtain first-order sensitivity of the  $J$ -integral for linear-elastic cracked structures. Since this method requires only the first-order sensitivity of a displacement field, it is simpler and more efficient than existing methods. Most of these methods, however, have been developed for mode-I loading conditions only. Although the bulk of fracture-mechanics literature is concerned with the first mode of crack deformation, there are practical engineering problems that involve mixed-mode conditions. Hence, there is a need to develop sensitivity equations for mixed-mode loading conditions.

This paper presents a new method for predicting the first-order sensitivity of mode-I and mode-II stress-intensity factors,  $K_I$  and  $K_{II}$ , respectively, for a crack in a homogeneous, isotropic, linear-elastic structure. The method involves the material derivative concept of continuum mechanics, domain integral representation of an interaction integral, known as the  $M$ -integral, and direct differentiation. Numerical examples are presented to calculate the first-order derivative of the  $M$ -integral and stress-intensity factors, using the proposed method. The results from this method are compared with analytical and finite-difference methods.

## 2 Shape sensitivity analysis

### 2.1 Velocity field

Consider a general three-dimensional body defined as an uncountable infinity of points, called material points, that can be mapped homeomorphically into the closure of open, connected subsets of the Euclidean vector space  $E^3$ . Each such homeomorphism defines a configuration of the body. Consider one particular configuration, a reference configuration, with domain  $\Omega \subset E^3$  and identify a material point of the body with its position vector  $x \in \Omega$ . Figure 1

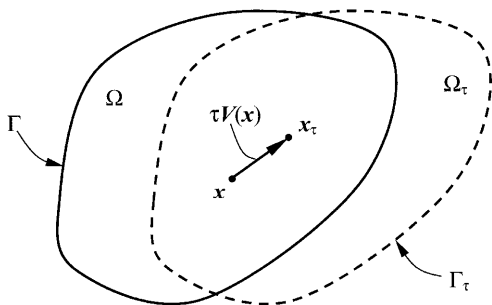


Fig. 1. Variation of domain

shows the motion of the body from a configuration with domain  $\Omega$  and boundary  $\Gamma$  into another configuration with domain  $\Omega_\tau$  and boundary  $\Gamma_\tau$ . This dynamic process can be represented by

$$\mathbf{T} : \mathbf{x} \rightarrow \mathbf{x}_\tau, \quad \mathbf{x} \in \Omega \quad (1)$$

where  $\mathbf{x}$  and  $\mathbf{x}_\tau$  are the position vectors of a material point in the reference and perturbed configurations, respectively,  $\mathbf{T}$  is a transformation mapping,  $\tau$  plays the role of time, with

$$\begin{aligned} \mathbf{x}_\tau &= \mathbf{T}(\mathbf{x}, \tau) \\ \Omega_\tau &= \mathbf{T}(\Omega, \tau) \\ \Gamma_\tau &= \mathbf{T}(\Gamma, \tau) \end{aligned} \quad (2)$$

A velocity field  $\mathbf{V}$  can then be defined as

$$\mathbf{V}(\mathbf{x}_\tau, \tau) = \frac{d\mathbf{x}_\tau}{d\tau} = \frac{d\mathbf{T}(\mathbf{x}, \tau)}{d\tau} = \frac{\partial \mathbf{T}(\mathbf{x}, \tau)}{\partial \tau} \quad (3)$$

In the neighborhood of the initial time  $\tau = 0$ , assuming a regularity hypothesis and ignoring higher-order terms,  $\mathbf{T}$  can be approximated by

$$\begin{aligned} \mathbf{T}(\mathbf{x}, \tau) &= \mathbf{T}(\mathbf{x}, 0) + \tau \frac{\partial \mathbf{T}(\mathbf{x}, 0)}{\partial \tau} + \mathbf{O}(\tau^2) \\ &\cong \mathbf{x} + \tau \mathbf{V}(\mathbf{x}, 0) \end{aligned} \quad (4)$$

where  $\mathbf{x} = \mathbf{T}(\mathbf{x}, 0)$  and  $\mathbf{V}(\mathbf{x}) = \mathbf{V}(\mathbf{x}, 0)$ .

### 2.2 Sensitivity analysis

The variational governing equation for a structural component with the domain  $\Omega$  can be written as [16, 18, 19]

$$a_\Omega(\mathbf{z}, \bar{\mathbf{z}}) = \ell_\Omega(\bar{\mathbf{z}}), \quad \text{for all } \bar{\mathbf{z}} \in \mathbf{Z} \quad (5)$$

where  $\mathbf{z}$  and  $\bar{\mathbf{z}}$  are the actual displacement and virtual displacement fields of the structure, respectively,  $\mathbf{Z}$  is the space of kinematically admissible virtual displacements, and  $a_\Omega(\mathbf{z}, \bar{\mathbf{z}})$  and  $\ell_\Omega(\bar{\mathbf{z}})$  are energy bilinear and load linear forms, respectively. The subscript  $\Omega$  in Eq. (5) is used to indicate the dependency of the governing equation on the shape of the structural domain.

The pointwise material derivative at  $\mathbf{x} \in \Omega$  is defined as [16–18]

$$\dot{\mathbf{z}} = \lim_{\tau \rightarrow 0} \left[ \frac{\mathbf{z}_\tau(\mathbf{x} + \tau \mathbf{V}(\mathbf{x})) - \mathbf{z}(\mathbf{x})}{\tau} \right] \quad (6)$$

If  $\mathbf{z}_\tau$  has a regular extension to a neighborhood of  $\Omega_\tau$ , then

$$\dot{\mathbf{z}}(\mathbf{x}) = \mathbf{z}'(\mathbf{x}) + \nabla \mathbf{z}^T \mathbf{V}(\mathbf{x}) \quad (7)$$

where

$$\mathbf{z}' = \lim_{\tau \rightarrow 0} \left[ \frac{\mathbf{z}_\tau(\mathbf{x}) - \mathbf{z}(\mathbf{x})}{\tau} \right] \quad (8)$$

is the partial derivative of  $\mathbf{z}$  and  $\nabla = \{\partial/\partial x_1, \partial/\partial x_2, \partial/\partial x_3\}^T$  is the vector of gradient operators. From Eq. (7),

$$\mathbf{z}'(\mathbf{x}) = \dot{\mathbf{z}}(\mathbf{x}) - \nabla \mathbf{z}^T \mathbf{V}(\mathbf{x}) \quad (9)$$

One attractive feature of the partial derivative is that, given a smoothness assumption, it commutes with the deriva-

tives with respect to  $x_i$ ,  $i = 1, 2$ , and  $3$ , since they are derivatives with respect to independent variables, i.e.,

$$\left(\frac{\partial \mathbf{z}}{\partial x_i}\right)' = \frac{\partial}{\partial x_i}(\mathbf{z}'), \quad i = 1, 2, \text{ and } 3. \quad (10)$$

Let  $\psi_1$  be a domain functional, defined as an integral over  $\Omega_\tau$ ,

$$\psi_1 = \int_{\Omega_\tau} f_\tau(\mathbf{x}_\tau) d\Omega_\tau \quad (11)$$

where  $f_\tau$  is a regular function defined on  $\Omega_\tau$ . If  $\Omega$  is  $C^k$  regular, then the material derivative of  $\psi_1$  at  $\Omega$  is [16, 18, 19]

$$\dot{\psi}_1 = \int_{\Omega} [f'(\mathbf{x}) + \text{div}(f(\mathbf{x})\mathbf{V}(\mathbf{x}))] d\Omega. \quad (12)$$

For a functional form of

$$\psi_2 = \int_{\Omega_\tau} g(\mathbf{z}_\tau, \mathbf{V}\mathbf{z}_\tau) d\Omega_\tau, \quad (13)$$

the material derivative of  $\psi_2$  at  $\Omega$  using Eqs. (10) and (12) is

$$\dot{\psi}_2 = \int_{\Omega} [\mathbf{g}_z \mathbf{z}' + \mathbf{g}_{\mathbf{V}\mathbf{z}} \mathbf{V}\mathbf{z}' + \text{div}(\mathbf{g}\mathbf{V})] d\Omega, \quad (14)$$

where  $\mathbf{g}_z = \{\partial g/\partial z_1, \partial g/\partial z_2, \partial g/\partial z_3\}^T$ , and

$$\mathbf{g}_{\mathbf{V}\mathbf{z}} = \begin{bmatrix} \frac{\partial g}{\partial(\partial z_1/\partial x_1)} & \frac{\partial g}{\partial(\partial z_1/\partial x_2)} & \frac{\partial g}{\partial(\partial z_1/\partial x_3)} \\ \frac{\partial g}{\partial(\partial z_2/\partial x_1)} & \frac{\partial g}{\partial(\partial z_2/\partial x_2)} & \frac{\partial g}{\partial(\partial z_2/\partial x_3)} \\ \frac{\partial g}{\partial(\partial z_3/\partial x_1)} & \frac{\partial g}{\partial(\partial z_3/\partial x_2)} & \frac{\partial g}{\partial(\partial z_3/\partial x_3)} \end{bmatrix}. \quad (15)$$

Using Eq. (9), Eq. (14) can be rewritten as

$$\dot{\psi}_2 = \int_{\Omega} [\mathbf{g}_z \dot{\mathbf{z}} - \mathbf{g}_z (\mathbf{V}\mathbf{z}^T \mathbf{V}) + \mathbf{g}_{\mathbf{V}\mathbf{z}} \mathbf{V}\dot{\mathbf{z}} - \mathbf{g}_{\mathbf{V}\mathbf{z}} \mathbf{V}(\mathbf{V}\mathbf{z}^T \mathbf{V}) + \text{div}(\mathbf{g}\mathbf{V})] d\Omega. \quad (16)$$

In Eq. (16), the material derivative  $\dot{\mathbf{z}}$  is the solution of the sensitivity equation obtained by taking the material derivative of Eq. (5).

If no body force is involved, the variational equation (Eq. 5) can be written as

$$a_\Omega(\mathbf{z}, \bar{\mathbf{z}}) \equiv \int_{\Omega} \sigma_{ij}(\mathbf{z}) \varepsilon_{ij}(\bar{\mathbf{z}}) d\Omega = \ell_\Omega(\bar{\mathbf{z}}) \equiv \int_{\Gamma} T_i \bar{z}_i d\Gamma \quad (17)$$

where  $\sigma_{ij}(\mathbf{z})$  and  $\varepsilon_{ij}(\bar{\mathbf{z}})$  are the stress and strain tensors of the displacement  $\mathbf{z}$  and virtual displacement  $\bar{\mathbf{z}}$ , respectively,  $T_i$  is the  $i$ th component of the surface traction, and  $\bar{z}_i$  is the  $i$ th component of  $\bar{\mathbf{z}}$ .

Taking the material derivative of both sides of Eq. (17), using Eq. (9), and noting that the partial derivatives with respect to  $\tau$  and  $x_i$  commute with each other,

$$a_\Omega(\dot{\mathbf{z}}, \bar{\mathbf{z}}) = \ell'_V(\bar{\mathbf{z}}) - a'_V(\mathbf{z}, \bar{\mathbf{z}}), \quad \forall \bar{\mathbf{z}} \in \mathbf{Z} \quad (18)$$

where the subscript  $\mathbf{V}$  is used to indicate the dependency of the terms on the velocity field. The terms  $\ell'_V(\bar{\mathbf{z}})$  and  $a'_V(\mathbf{z}, \bar{\mathbf{z}})$  can be further derived as

$$\ell'_V(\bar{\mathbf{z}}) = \int_{\Gamma} \{ -T_i(z_{i,j} V_j) + [(T_i \bar{z}_i)_{,j} n_j + \kappa_\Gamma (T_i \bar{z}_i)] (V_i n_i) \} d\Gamma \quad (19)$$

and

$$a'_V(\mathbf{z}, \bar{\mathbf{z}}) = - \int_{\Omega} [\sigma_{ij}(\mathbf{z}) (\bar{z}_{i,k} V_{k,j}) + \sigma_{ij}(\bar{\mathbf{z}}) (z_{i,k} V_{k,j}) - \sigma_{ij}(\mathbf{z}) \varepsilon_{ij}(\bar{\mathbf{z}}) \text{div} \mathbf{V}] d\Omega \quad (20)$$

where  $V_i$  is the  $i$ th component of  $\mathbf{V}$ ,  $n_i$  is the  $i$ th component of unit normal vector  $\mathbf{n}$ , and  $\kappa_\Gamma$  is the curvature of the boundary, and  $z_{i,j} = \partial z_i/\partial x_j$ ,  $\bar{z}_{i,j} = \partial \bar{z}_i/\partial x_j$ ,  $V_{i,j} = \partial V_i/\partial x_j$ .

To evaluate the sensitivity expression of Eq. (16), a numerical method is needed to solve Eq. (17). In this study, the standard FEM was used. If the solution  $\mathbf{z}$  of Eq. (17) is obtained using an FEM code, the same code can be used to solve Eq. (18) for  $\dot{\mathbf{z}}$ . This solution of  $\dot{\mathbf{z}}$  can be obtained efficiently, since it requires only the evaluation of the same set of FEM matrix equations with a different fictitious load, i.e., the right hand side of Eq. (18). In this study, the ABAQUS (Version 5.8) [20] finite element code was used in all numerical calculations, as presented in forthcoming sections.

### 3

#### The interaction integral and its sensitivity

##### 3.1

##### The interaction integral

Consider a structure with a rectilinear crack of length  $2a$  and orientation  $\gamma$ , subjected to external loads  $S_1, S_2, \dots, S_m$ , as shown in Fig. 2. The structure is subjected to mixed-mode deformation involving primary modes I and II. Let  $K_I$  and  $K_{II}$  be the SIFs for mode-I and mode-II, respectively. The SIFs can be calculated using the interaction integral [21] converted into a domain form [22, 23]. For example,  $K_I$  can be calculated from

$$K_I = \frac{E'}{2} M^{(1,2)} \quad (21)$$

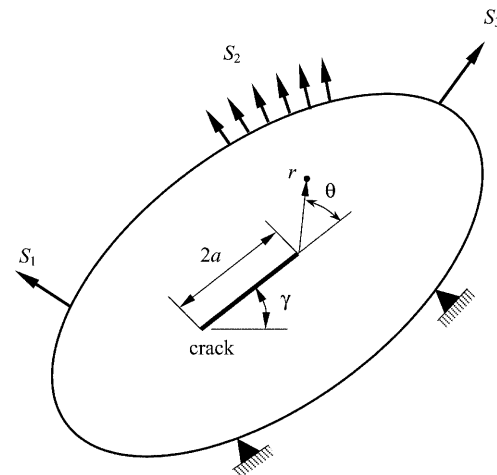


Fig. 2. General cracked body under mixed-mode loading

where

$$E' = \begin{cases} E, & \text{plane stress} \\ \frac{E}{1-\nu^2}, & \text{plane strain} \end{cases}, \quad (22)$$

is the effective elastic modulus with  $E$  and  $\nu$  representing the modulus of elasticity and Poisson's ratio, respectively, and  $M^{(1,2)}$  is the interaction integral defined as

$$M^{(1,2)} = \int_A \left[ \sigma_{ij}^{(1)} \frac{\partial z_i^{(2)}}{\partial x_1} + \sigma_{ij}^{(2)} \frac{\partial z_i^{(1)}}{\partial x_1} - W^{(1,2)} \delta_{1j} \right] \frac{\partial q}{\partial x_j} dA \quad (23)$$

where  $\sigma_{ij}$  and  $z_i$  are the components of stress tensor and displacement vector, respectively,

$$W^{(1,2)} = \frac{1}{2} \left[ \sigma_{ij}^{(1)} \varepsilon_{ij}^{(2)} + \sigma_{ij}^{(2)} \varepsilon_{ij}^{(1)} \right] = \sigma_{ij}^{(1)} \varepsilon_{ij}^{(2)} = \sigma_{ij}^{(2)} \varepsilon_{ij}^{(1)} \quad (24)$$

is the mutual strain energy from the two states,  $A$  is the domain area inside an arbitrarily chosen counter-clockwise contour around the crack tip, and  $q$  is a weight function chosen such that it has a value of unity at the crack tip, zero along the boundary of the domain, and arbitrary elsewhere. Equations (23) and (24) include the terms from the actual mixed-mode state for the given loading and boundary conditions (superscript 1) and the superimposed near-tip mode-I auxiliary state corresponding to unit SIF (superscript 2). The mode-I auxiliary state for stresses and displacements for a unit SIF can be written as

$$\begin{Bmatrix} \sigma_{11} \\ \sigma_{22} \\ \sigma_{12} \end{Bmatrix} = \frac{1}{\sqrt{2\pi r}} \begin{Bmatrix} \cos \frac{\theta}{2} \left( 1 - \sin \frac{\theta}{2} \sin \frac{3\theta}{2} \right) \\ \cos \frac{\theta}{2} \left( 1 + \sin \frac{\theta}{2} \sin \frac{3\theta}{2} \right) \\ \cos \frac{\theta}{2} \sin \frac{\theta}{2} \cos \frac{3\theta}{2} \end{Bmatrix} \quad (25)$$

and

$$\begin{Bmatrix} z_1 \\ z_2 \end{Bmatrix} = \frac{1}{2\mu} \sqrt{\frac{r}{2\pi}} \begin{Bmatrix} \cos \frac{\theta}{2} \left[ \kappa - 1 + 2 \sin^2 \frac{\theta}{2} \right] \\ \sin \frac{\theta}{2} \left[ \kappa + 1 - 2 \cos^2 \frac{\theta}{2} \right] \end{Bmatrix}, \quad (26)$$

respectively, where  $\mu$  is the shear modulus and  $\kappa = (3 - \nu)/(1 + \nu)$  for plane stress and  $\kappa = 3 - 4\nu$  for plane strain. Note all quantities are evaluated with respect to a coordinate system with the crack tip as the origin. Here, the summation convention is adopted for repeated indices.

Following a similar treatment,  $K_{II}$  can be also calculated from

$$K_{II} = \frac{E'}{2} M^{(1,2)} \quad (27)$$

and equations similar to Eqs. (22)–(24), except that the mode II auxiliary state for stresses and displacements for a unit SIF should be used, which are

$$\begin{Bmatrix} \sigma_{11} \\ \sigma_{22} \\ \sigma_{12} \end{Bmatrix} = \frac{1}{\sqrt{2\pi r}} \begin{Bmatrix} -\sin \frac{\theta}{2} \left[ 2 + \cos \frac{\theta}{2} \cos \frac{3\theta}{2} \right] \\ \sin \frac{\theta}{2} \cos \frac{\theta}{2} \cos \frac{3\theta}{2} \\ \cos \frac{\theta}{2} \left[ 1 - \sin \frac{\theta}{2} \sin \frac{3\theta}{2} \right] \end{Bmatrix} \quad (28)$$

and

$$\begin{Bmatrix} z_1 \\ z_2 \end{Bmatrix} = \frac{1}{2\mu} \sqrt{\frac{r}{2\pi}} \begin{Bmatrix} \sin \frac{\theta}{2} \left[ \kappa + 1 + 2 \cos^2 \frac{\theta}{2} \right] \\ -\cos \frac{\theta}{2} \left[ \kappa - 1 - 2 \sin^2 \frac{\theta}{2} \right] \end{Bmatrix}. \quad (29)$$

## 3.2

### Sensitivity of interaction integral and stress-intensity factors

#### 3.2.1

##### Sensitivity of interaction integral

Expanding each term of Eq. (23) yields

$$\begin{aligned} \sigma_{ij}^{(1)} \frac{\partial z_i^{(2)}}{\partial x_1} \frac{\partial q}{\partial x_j} &= \sigma_{11}^{(1)} \frac{\partial z_1^{(2)}}{\partial x_1} \frac{\partial q}{\partial x_1} + \sigma_{12}^{(1)} \frac{\partial z_1^{(2)}}{\partial x_1} \frac{\partial q}{\partial x_2} \\ &+ \sigma_{21}^{(1)} \frac{\partial z_2^{(2)}}{\partial x_1} \frac{\partial q}{\partial x_1} + \sigma_{22}^{(1)} \frac{\partial z_2^{(2)}}{\partial x_1} \frac{\partial q}{\partial x_2} \end{aligned} \quad (30)$$

$$\begin{aligned} \sigma_{ij}^{(2)} \frac{\partial z_i^{(1)}}{\partial x_1} \frac{\partial q}{\partial x_j} &= \sigma_{11}^{(2)} \frac{\partial z_1^{(1)}}{\partial x_1} \frac{\partial q}{\partial x_1} + \sigma_{12}^{(2)} \frac{\partial z_1^{(1)}}{\partial x_1} \frac{\partial q}{\partial x_2} \\ &+ \sigma_{21}^{(2)} \frac{\partial z_2^{(1)}}{\partial x_1} \frac{\partial q}{\partial x_1} + \sigma_{22}^{(2)} \frac{\partial z_2^{(1)}}{\partial x_1} \frac{\partial q}{\partial x_2} \end{aligned} \quad (31)$$

and

$$\begin{aligned} W^{(1,2)} \delta_{1j} \frac{\partial q}{\partial x_j} &= \left[ \sigma_{11}^{(2)} \frac{\partial z_1^{(1)}}{\partial x_1} + \sigma_{12}^{(2)} \left( \frac{\partial z_1^{(1)}}{\partial x_2} + \frac{\partial z_2^{(1)}}{\partial x_1} \right) \right. \\ &\left. + \sigma_{22}^{(2)} \frac{\partial z_2^{(1)}}{\partial x_2} \right] \frac{\partial q}{\partial x_1}. \end{aligned} \quad (32)$$

Applying Eqs. (30)–(32) in Eq. (23) yields

$$\begin{aligned} M^{(1,2)} &= \int_A \left[ \sigma_{11}^{(1)} \frac{\partial z_1^{(2)}}{\partial x_1} \frac{\partial q}{\partial x_1} + \sigma_{12}^{(1)} \frac{\partial z_1^{(2)}}{\partial x_1} \frac{\partial q}{\partial x_2} \right. \\ &+ \sigma_{21}^{(1)} \frac{\partial z_2^{(2)}}{\partial x_1} \frac{\partial q}{\partial x_1} + \sigma_{22}^{(1)} \frac{\partial z_2^{(2)}}{\partial x_1} \frac{\partial q}{\partial x_2} \Big] dA \\ &+ \int_A \left[ \sigma_{12}^{(2)} \frac{\partial z_1^{(1)}}{\partial x_1} \frac{\partial q}{\partial x_2} + \sigma_{22}^{(2)} \frac{\partial z_2^{(1)}}{\partial x_1} \frac{\partial q}{\partial x_2} \right. \\ &\left. - \sigma_{12}^{(2)} \frac{\partial z_1^{(1)}}{\partial x_2} \frac{\partial q}{\partial x_1} - \sigma_{22}^{(2)} \frac{\partial z_2^{(1)}}{\partial x_2} \frac{\partial q}{\partial x_1} \right] dA. \end{aligned} \quad (33)$$

For the two-dimensional plane stress or plane strain problem, once the stress–strain relationship is applied, Eq. (33) can be expressed as

$$M^{(1,2)} = \int_A h dA \quad (34)$$

where

$$h = h_1 + h_2 + h_3 + h_4 + h_5 + h_6 - h_7 - h_8 \quad (35)$$

with  $h_i$ ,  $i = 1, \dots, 8$  dependent on the state of stress.

For plane stress,

$$h_1 = \frac{E}{1-\nu^2} \left( \frac{\partial z_1^{(1)}}{\partial x_1} + \nu \frac{\partial z_2^{(1)}}{\partial x_2} \right) \frac{\partial z_1^{(2)}}{\partial x_1} \frac{\partial q}{\partial x_1} \quad (36)$$

$$h_2 = \frac{E}{2(1+\nu)} \left( \frac{\partial z_1^{(1)}}{\partial x_2} + \frac{\partial z_2^{(1)}}{\partial x_1} \right) \frac{\partial z_1^{(2)}}{\partial x_1} \frac{\partial q}{\partial x_1} \quad (37)$$

$$h_3 = \frac{E}{2(1+\nu)} \left( \frac{\partial z_1^{(1)}}{\partial x_2} + \frac{\partial z_2^{(1)}}{\partial x_1} \right) \frac{\partial z_2^{(2)}}{\partial x_1} \frac{\partial q}{\partial x_1} \quad (38)$$

$$h_4 = \frac{E}{1-\nu^2} \left( \nu \frac{\partial z_1^{(1)}}{\partial x_1} + \frac{\partial z_2^{(1)}}{\partial x_2} \right) \frac{\partial z_2^{(2)}}{\partial x_1} \frac{\partial q}{\partial x_2} \quad (39)$$

$$h_5 = \sigma_{12}^{(2)} \frac{\partial z_1^{(1)}}{\partial x_1} \frac{\partial q}{\partial x_2} \quad (40)$$

$$h_6 = \sigma_{22}^{(2)} \frac{\partial z_2^{(1)}}{\partial x_1} \frac{\partial q}{\partial x_2} \quad (41)$$

$$h_7 = \sigma_{12}^{(2)} \frac{\partial z_1^{(1)}}{\partial x_2} \frac{\partial q}{\partial x_1} \quad (42)$$

$$h_8 = \sigma_{22}^{(2)} \frac{\partial z_2^{(1)}}{\partial x_2} \frac{\partial q}{\partial x_1} \quad (43)$$

For plane strain,

$$h_1 = \frac{E}{(1+\nu)(1-2\nu)} \left[ (1-\nu) \frac{\partial z_1^{(1)}}{\partial x_1} + \nu \frac{\partial z_2^{(1)}}{\partial x_2} \right] \frac{\partial z_1^{(2)}}{\partial x_1} \frac{\partial q}{\partial x_1} \quad (44)$$

$$h_2 = \frac{E}{2(1+\nu)} \left( \frac{\partial z_1^{(1)}}{\partial x_2} + \frac{\partial z_2^{(1)}}{\partial x_1} \right) \frac{\partial z_1^{(2)}}{\partial x_1} \frac{\partial q}{\partial x_1} \quad (45)$$

$$h_3 = \frac{E}{2(1+\nu)} \left( \frac{\partial z_1^{(1)}}{\partial x_2} + \frac{\partial z_2^{(1)}}{\partial x_1} \right) \frac{\partial z_2^{(2)}}{\partial x_1} \frac{\partial q}{\partial x_1} \quad (46)$$

$$h_4 = \frac{E}{(1+\nu)(1-2\nu)} \left[ \nu \frac{\partial z_1^{(1)}}{\partial x_1} + (1-\nu) \frac{\partial z_2^{(1)}}{\partial x_2} \right] \frac{\partial z_2^{(2)}}{\partial x_1} \frac{\partial q}{\partial x_2} \quad (47)$$

$$h_5 = \sigma_{12}^{(2)} \frac{\partial z_1^{(1)}}{\partial x_1} \frac{\partial q}{\partial x_2} \quad (48)$$

$$h_6 = \sigma_{22}^{(2)} \frac{\partial z_2^{(1)}}{\partial x_1} \frac{\partial q}{\partial x_2} \quad (49)$$

$$h_7 = \sigma_{12}^{(2)} \frac{\partial z_1^{(1)}}{\partial x_2} \frac{\partial q}{\partial x_1} \quad (50)$$

$$h_8 = \sigma_{22}^{(2)} \frac{\partial z_2^{(1)}}{\partial x_2} \frac{\partial q}{\partial x_1} \quad (51)$$

Hence, in relation to Eq. (12), the material derivative of  $M^{(1,2)}$  is

$$\dot{M}^{(1,2)} = \int_A [h' + \text{div}(hV)] dA \quad (52)$$

where,

$$h' = h'_1 + h'_2 + h'_3 + h'_4 + h'_5 + h'_6 - h'_7 - h'_8 \quad (53)$$

$$\mathbf{V} = \begin{Bmatrix} V_1 \\ V_2 \end{Bmatrix} \quad (54)$$

and

$$\begin{aligned} \text{div}(hV) &= \frac{\partial(hV_1)}{\partial x_1} + \frac{\partial(hV_2)}{\partial x_2} \\ &= \frac{\partial(h_1V_1)}{\partial x_1} + \frac{\partial(h_2V_1)}{\partial x_1} + \frac{\partial(h_3V_1)}{\partial x_1} + \frac{\partial(h_4V_1)}{\partial x_1} \\ &\quad + \frac{\partial(h_5V_1)}{\partial x_1} + \frac{\partial(h_6V_1)}{\partial x_1} - \frac{\partial(h_7V_1)}{\partial x_1} - \frac{\partial(h_8V_1)}{\partial x_1} \\ &\quad + \frac{\partial(h_1V_2)}{\partial x_1} + \frac{\partial(h_2V_2)}{\partial x_1} + \frac{\partial(h_3V_2)}{\partial x_1} + \frac{\partial(h_4V_2)}{\partial x_1} \\ &\quad + \frac{\partial(h_5V_2)}{\partial x_1} + \frac{\partial(h_6V_2)}{\partial x_1} - \frac{\partial(h_7V_2)}{\partial x_1} - \frac{\partial(h_8V_2)}{\partial x_1} \end{aligned} \quad (55)$$

Equation (52) then becomes

$$\dot{M}^{(1,2)} = \int_A (H_1 + H_2 + H_3 + H_4 + H_5 + H_6 - H_7 - H_8) dA \quad (56)$$

where

$$H_i = h'_i + \frac{\partial(h_iV_1)}{\partial x_1} + \frac{\partial(h_iV_2)}{\partial x_2}, \quad i = 1, \dots, 8 \quad (57)$$

The explicit expressions of  $H_i$ ,  $i = 1, \dots, 8$  are given in Appendix A for both plane stress and plane strain conditions.

Equations (A1)–(A8) and (A9)–(A16) in Appendix A provide explicit expressions of  $H_i$ ,  $i = 1, 8$  for plane stress and plane strain conditions, respectively, which can be inserted in Eq. (56) to yield the first-order sensitivity of  $M^{(1,2)}$  with respect to crack size. The integral in Eq. (56) is independent of the domain size  $A$  and can be calculated numerically using standard Gaussian quadrature. A  $2 \times 2$  or higher integration rule is recommended for calculating  $\dot{M}$ . A flow diagram for calculating the sensitivity of  $M$  is shown in Fig. 3.

### 3.2.2

#### Sensitivities of stress-intensity factors

From Eqs. (21) and (27), the sensitivities of  $K_I$  and  $K_{II}$  can be calculated by

$$\frac{\partial K_I}{\partial a} = \frac{E'}{2} \frac{\partial M^{(1,I)}}{\partial a} \quad (58)$$

$$\frac{\partial K_{II}}{\partial a} = \frac{E'}{2} \frac{\partial M^{(1,II)}}{\partial a} \quad (59)$$

where  $M^{(1,I)}$  and  $M^{(1,II)}$  are the interaction integrals for mode-I and mode-II, respectively.

## 4

### Numerical examples

#### 4.1

##### Example 1: Angle-cracked plate under far-field tension

Consider a cracked plate with width  $2W = 20$  units, length  $2L = 20$  units, and two cases of crack length  $2a$ , with  $a/W = 0.05$  and  $a/W = 0.1$ , subjected to a far-field remote tensile stress  $\sigma^\infty = 1$  unit. The material properties, the elastic modulus  $E = 26$  units, Poisson's ratio  $\nu = 0.3$ ,

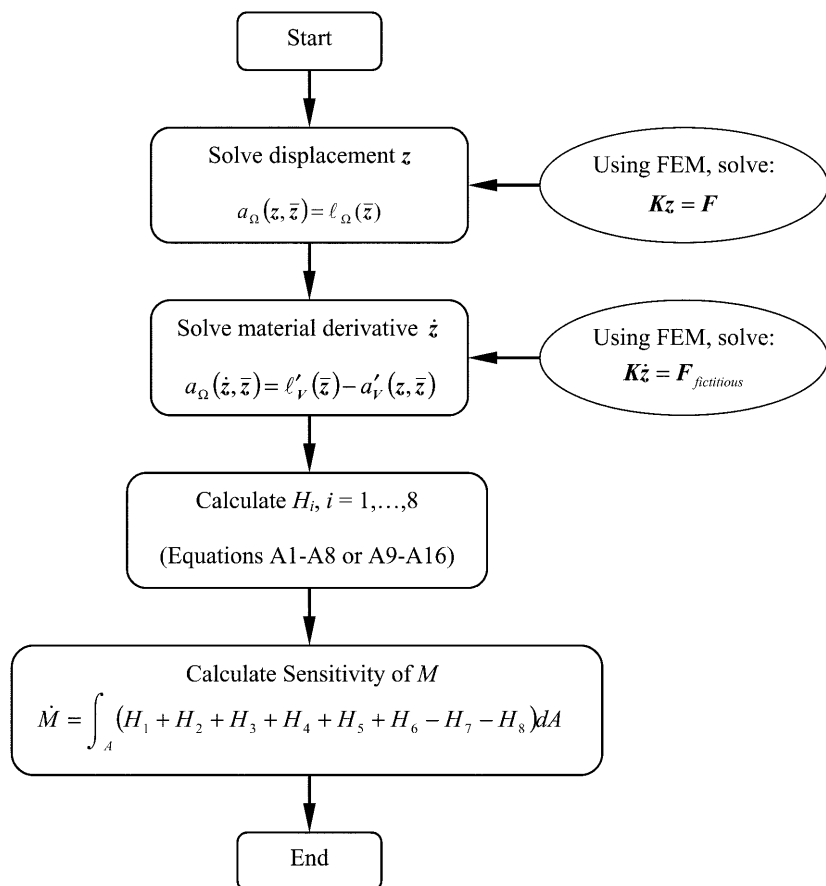


Fig. 3. A flowchart for continuum sensitivity analysis of crack size

and the crack orientation angle  $\gamma = 45^\circ$  were selected. A plane stress condition was assumed.

Figure 4a shows the geometry and load of the cracked panel. A finite element mesh for this problem with  $a/W = 0.1$  is shown in Fig. 4b. Second-order elements from the ABAQUS (Version 5.8) [20] element library were used. The element type was CPS8R, a reduced integration, eight-noded quadrilateral element. The number of elements and nodes were 656 and 1400, respectively. A ring of 32 focused elements with collapsed nodes was employed in the vicinity of the crack tip. The size of the integral domain was  $2b_1 = 2b_2 = 2a$ , as shown in Fig. 4a. A  $2 \times 2$  Gaussian integration scheme was used to calculate the sensitivities.

The analytical solutions of  $K_I$  and  $K_{II}$  for an infinite panel ( $a/W \rightarrow 0$ ) under this loading condition are [24],

$$K_I = \sigma^\infty \sin^2 \gamma \sqrt{\pi a} \quad (60)$$

and

$$K_{II} = \sigma^\infty \sin \gamma \cos \gamma \sqrt{\pi a} \quad (61)$$

Hence, their derivatives with respect to crack length are

$$\frac{\partial K_I}{\partial a} = \frac{1}{2} \sigma^\infty \sin^2 \gamma \sqrt{\frac{\pi}{a}} \quad (62)$$

and

$$\frac{\partial K_{II}}{\partial a} = \frac{1}{2} \sigma^\infty \sin \gamma \cos \gamma \sqrt{\frac{\pi}{a}} \quad (63)$$

Table 1 shows the numerical results for  $\partial K_I / \partial a$  and  $\partial K_{II} / \partial a$  using two methods, one of which is based on the proposed continuum shape sensitivity method described

in this paper. The other method is based on the exact solution of an infinite panel [i.e., Eqs. (62) and (63)]. The results in Table 1 show that the continuum shape sensitivity method is accurate for computation of  $\partial K_I / \partial a$  and  $\partial K_{II} / \partial a$ , when compared with the corresponding results of the infinite panel. The difference between the results of the proposed method and the infinite-panel solution is less than 2 and 4 percent for modes I and II, respectively.

## 4.2

### Example 2: Edge-cracked plate under far-field shear

This example involves an edge-cracked plate, as shown in Fig. 5a, fixed at the bottom and subjected to a far-field shear stress  $\tau^\infty = 1$  unit applied at the top. The plate has length  $L = 16$  units, width  $W = 7$  units, and two cases of crack length,  $a = 1.75$  and 3.5 units. A  $2b_1 \times 2b_2$  domain with  $2b_1 = 2b_2 = 3.5$  units, required to calculate the  $M^{(1,2)}$  integral, is also shown in Fig. 5a. Figure 5b shows the finite element discretization for  $a = 3.5$  units, which involves 1235 nodes and 560 elements. A ring of 32 focused elements with collapsed nodes was used in the crack-tip region. The elastic modulus and Poisson's ratio were  $30 \times 10^6$  units and 0.25, respectively. A plane strain condition was assumed.

Table 2 shows the numerical results for  $\partial K_I / \partial a$  and  $\partial K_{II} / \partial a$  using the proposed continuum shape sensitivity method. Since no analytical solutions were available for this problem, the finite-difference method with a one-percent crack-length perturbation was selected to verify the results of the proposed method. The results in Table 2 show that the continuum shape sensitivity method

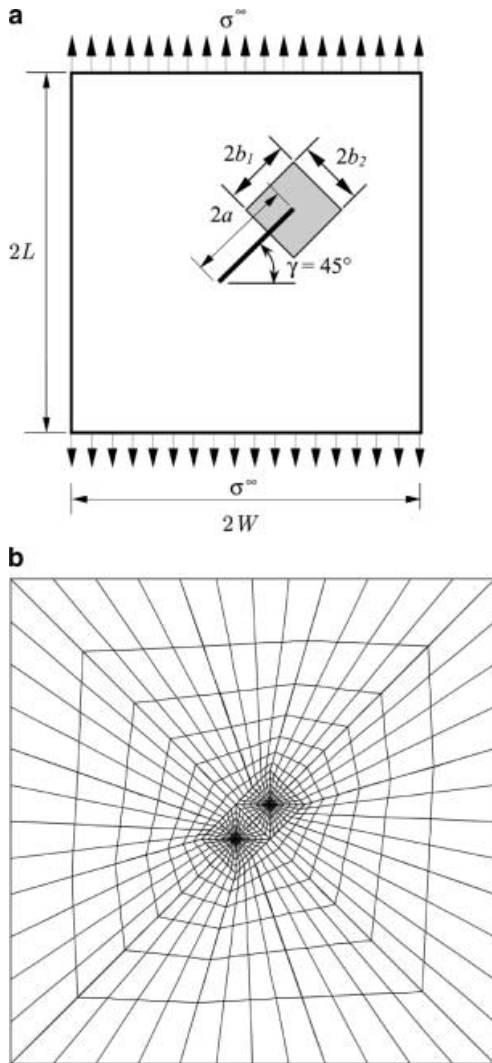


Fig. 4a, b. Angle-cracked plate under remote tension a geometry and loads; b finite element mesh for  $a/W = 0.1$  (full model)

Table 1. Sensitivity of  $K_I$  and  $K_{II}$  for angle-cracked specimen by the proposed method and analytical solution

$a/W$	SIF ( $K_I, K_{II}$ )	Sensitivity of SIF ( $\partial K_I/\partial a, \partial K_{II}/\partial a$ )		Difference <sup>a</sup> percent
		Proposed method	Analytical solution	
<b>Mode-I</b>				
0.05	0.6298	0.6297	0.6267	-0.49
0.1	0.8729	0.4350	0.4431	1.80
<b>Mode-II</b>				
0.05	0.6091	0.6078	0.6267	3.0
0.1	0.8552	0.4265	0.4431	3.8

<sup>a</sup> Difference = (analytical solution – proposed method)  $\times$  100/analytical solution

provides accurate estimates for  $\partial K_I/\partial a$  and  $\partial K_{II}/\partial a$  when compared with the corresponding results of the finite-difference method. The difference between the results of the proposed and finite-difference methods is less than 4%.

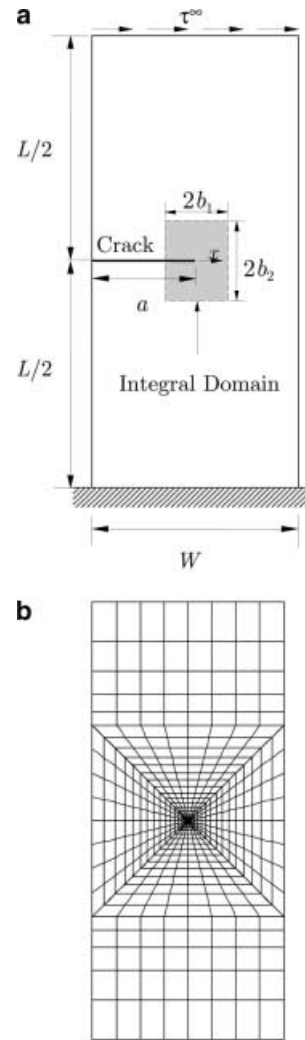


Fig. 5a, b. Edge-cracked plate under remote shear a geometry and loads; b finite element mesh for  $a/W = 0.5$  (full model)

Table 2. Sensitivity of  $K_I$  and  $K_{II}$  for edge-cracked specimen by the proposed and finite-difference methods

$a/W$	SIF ( $K_I, K_{II}$ )	Sensitivity of SIF ( $\partial K_I/\partial a, \partial K_{II}/\partial a$ )		Difference <sup>a</sup> percent
		Proposed method	Finite-difference method	
<b>Mode-I</b>				
0.25	17.44	6.60	6.54	-0.92
0.5	34.13	15.13	14.94	-1.45
<b>Mode-II</b>				
0.25	1.97	1.41	1.44	2.08
0.5	4.54	1.59	1.53	-3.77

<sup>a</sup> Difference = (finite-difference method – proposed method)  $\times$  100/finite-difference method

## 5 Summary and conclusions

A new method has been developed for continuum-based shape sensitivity analysis of a crack in a homogeneous,

isotropic, linear-elastic body subject to mixed-mode loading conditions. The method involves the material derivative concept of continuum mechanics, domain integral representation of an interaction integral, and direct differentiation. Unlike virtual crack extension techniques, no mesh perturbation is required in the proposed method to calculate the sensitivity of stress-intensity factors. Since the governing variational equation is differentiated prior to discretization, the resulting sensitivity equations are independent of approximate numerical techniques, such as the FEM, the boundary element method, meshless methods, or others. Also, since the proposed method requires only the first-order sensitivity of a displacement field, it is much simpler and more efficient than existing methods. Two numerical examples have been presented to illustrate the proposed method. The results show that the maximum difference between the sensitivity of stress-intensity factors calculated using the proposed method and reference solutions obtained by analytical or finite-difference methods is less than 4%.

## Appendix A

### Plane stress

$$\begin{aligned}
H_1 = & \frac{E}{1-\nu^2} \frac{\partial z_1^{(2)}}{\partial x_1} \frac{\partial q}{\partial x_1} \left[ \frac{\partial \dot{z}_1^{(1)}}{\partial x_1} + \nu \frac{\partial \dot{z}_2^{(1)}}{\partial x_2} \right. \\
& \left. - \left( \frac{\partial z_1^{(1)}}{\partial x_2} \frac{\partial V_2}{\partial x_1} + \nu \frac{\partial z_2^{(1)}}{\partial x_1} \frac{\partial V_1}{\partial x_2} \right) \right] \\
& + \frac{E}{1-\nu^2} \frac{\partial q}{\partial x_1} \left( \frac{\partial z_1^{(1)}}{\partial x_1} + \nu \frac{\partial z_2^{(1)}}{\partial x_2} \right) \left( \frac{\partial^2 z_1^{(2)}}{\partial x_1^2} V_1 + \frac{\partial^2 z_1^{(2)}}{\partial x_1 \partial x_2} V_2 \right) \\
& + \frac{E}{1-\nu^2} \frac{\partial z_1^{(2)}}{\partial x_1} \left( \frac{\partial z_1^{(1)}}{\partial x_1} + \nu \frac{\partial z_2^{(1)}}{\partial x_2} \right) \left( \frac{\partial^2 q}{\partial x_1^2} V_1 + \frac{\partial^2 q}{\partial x_1 \partial x_2} V_2 \right) \\
& + \frac{E}{1-\nu^2} \frac{\partial z_1^{(2)}}{\partial x_1} \frac{\partial q}{\partial x_1} \left( \nu \frac{\partial z_2^{(1)}}{\partial x_2} \frac{\partial V_1}{\partial x_1} + \frac{\partial z_1^{(1)}}{\partial x_1} \frac{\partial V_2}{\partial x_2} \right) \quad (A1)
\end{aligned}$$

$$\begin{aligned}
H_2 = & \frac{E}{2(1+\nu)} \frac{\partial z_1^{(2)}}{\partial x_1} \frac{\partial q}{\partial x_2} \left( \frac{\partial \dot{z}_1^{(1)}}{\partial x_2} + \frac{\partial \dot{z}_2^{(1)}}{\partial x_1} \right. \\
& \left. - \frac{\partial z_1^{(1)}}{\partial x_1} \frac{\partial V_1}{\partial x_2} - \frac{\partial z_2^{(1)}}{\partial x_2} \frac{\partial V_2}{\partial x_1} \right) \\
& + \frac{E}{2(1+\nu)} \frac{\partial q}{\partial x_2} \left( \frac{\partial z_1^{(1)}}{\partial x_2} + \frac{\partial z_2^{(1)}}{\partial x_1} \right) \left( \frac{\partial^2 z_1^{(2)}}{\partial x_1^2} V_1 + \frac{\partial^2 z_1^{(2)}}{\partial x_1 \partial x_2} V_2 \right) \\
& + \frac{E}{2(1+\nu)} \frac{\partial z_1^{(2)}}{\partial x_1} \left( \frac{\partial z_1^{(1)}}{\partial x_2} + \frac{\partial z_2^{(1)}}{\partial x_1} \right) \left( \frac{\partial^2 q}{\partial x_1 \partial x_2} V_1 + \frac{\partial^2 q}{\partial x_2^2} V_2 \right) \\
& + \frac{E}{2(1+\nu)} \frac{\partial z_1^{(2)}}{\partial x_1} \frac{\partial q}{\partial x_2} \left( \frac{\partial z_1^{(1)}}{\partial x_2} \frac{\partial V_1}{\partial x_1} + \frac{\partial z_2^{(1)}}{\partial x_1} \frac{\partial V_2}{\partial x_2} \right) \quad (A2)
\end{aligned}$$

$$\begin{aligned}
H_3 = & \frac{E}{2(1+\nu)} \frac{\partial z_2^{(2)}}{\partial x_1} \frac{\partial q}{\partial x_1} \left( \frac{\partial \dot{z}_1^{(1)}}{\partial x_2} + \frac{\partial \dot{z}_2^{(1)}}{\partial x_1} \right. \\
& \left. - \frac{\partial z_1^{(1)}}{\partial x_1} \frac{\partial V_1}{\partial x_2} + \frac{\partial z_2^{(1)}}{\partial x_2} \frac{\partial V_2}{\partial x_1} \right) \\
& + \frac{E}{2(1+\nu)} \frac{\partial q}{\partial x_1} \left( \frac{\partial z_1^{(1)}}{\partial x_2} + \frac{\partial z_2^{(1)}}{\partial x_1} \right) \left( \frac{\partial^2 z_2^{(2)}}{\partial x_1^2} V_1 + \frac{\partial^2 z_2^{(2)}}{\partial x_1 \partial x_2} V_2 \right) \\
& + \frac{E}{2(1+\nu)} \frac{\partial z_2^{(2)}}{\partial x_1} \left( \frac{\partial z_1^{(1)}}{\partial x_2} + \frac{\partial z_2^{(1)}}{\partial x_1} \right) \left( \frac{\partial^2 q}{\partial x_1^2} V_1 + \frac{\partial^2 q}{\partial x_1 \partial x_2} V_2 \right) \\
& + \frac{E}{2(1+\nu)} \frac{\partial z_2^{(2)}}{\partial x_1} \frac{\partial q}{\partial x_1} \left( \frac{\partial z_1^{(1)}}{\partial x_2} \frac{\partial V_1}{\partial x_1} + \frac{\partial z_2^{(1)}}{\partial x_1} \frac{\partial V_2}{\partial x_2} \right) \quad (A3)
\end{aligned}$$

$$\begin{aligned}
H_4 = & \frac{E}{1-\nu^2} \frac{\partial z_2^{(2)}}{\partial x_1} \frac{\partial q}{\partial x_2} \left[ \nu \frac{\partial \dot{z}_1^{(1)}}{\partial x_1} + \frac{\partial \dot{z}_2^{(1)}}{\partial x_2} \right. \\
& \left. - \left( \nu \frac{\partial z_1^{(1)}}{\partial x_2} \frac{\partial V_2}{\partial x_1} + \frac{\partial z_2^{(1)}}{\partial x_1} \frac{\partial V_1}{\partial x_2} \right) \right] \\
& + \frac{E}{1-\nu^2} \frac{\partial q}{\partial x_2} \left( \nu \frac{\partial z_1^{(1)}}{\partial x_1} + \frac{\partial z_2^{(1)}}{\partial x_2} \right) \left( \frac{\partial^2 z_2^{(2)}}{\partial x_1^2} V_1 + \frac{\partial^2 z_2^{(2)}}{\partial x_1 \partial x_2} V_2 \right) \\
& + \frac{E}{1-\nu^2} \frac{\partial z_2^{(2)}}{\partial x_1} \left( \nu \frac{\partial z_1^{(1)}}{\partial x_1} + \frac{\partial z_2^{(1)}}{\partial x_2} \right) \left( \frac{\partial^2 q}{\partial x_1 \partial x_2} V_1 + \frac{\partial^2 q}{\partial x_2^2} V_2 \right) \\
& + \frac{E}{1-\nu^2} \frac{\partial z_2^{(2)}}{\partial x_1} \frac{\partial q}{\partial x_2} \left( \nu \frac{\partial z_1^{(1)}}{\partial x_1} \frac{\partial V_2}{\partial x_2} + \frac{\partial z_2^{(1)}}{\partial x_2} \frac{\partial V_1}{\partial x_1} \right) \quad (A4)
\end{aligned}$$

$$\begin{aligned}
H_5 = & \sigma_{12}^{(2)} \frac{\partial q}{\partial x_2} \left( \frac{\partial \dot{z}_1^{(1)}}{\partial x_1} - \frac{\partial z_1^{(1)}}{\partial x_2} \frac{\partial V_2}{\partial x_1} \right) \\
& + \frac{\partial z_1^{(1)}}{\partial x_1} \frac{\partial q}{\partial x_2} \left( \frac{\partial \sigma_{12}^{(2)}}{\partial x_1} V_1 + \frac{\partial \sigma_{12}^{(2)}}{\partial x_2} V_2 \right) \\
& + \sigma_{12}^{(2)} \frac{\partial z_1^{(1)}}{\partial x_1} \left( \frac{\partial^2 q}{\partial x_1 \partial x_2} V_1 + \frac{\partial^2 q}{\partial x_2^2} V_2 \right) \\
& + \sigma_{12}^{(2)} \frac{\partial z_1^{(1)}}{\partial x_1} \frac{\partial q}{\partial x_2} \frac{\partial V_2}{\partial x_2} \quad (A5)
\end{aligned}$$

$$\begin{aligned}
H_6 = & \sigma_{22}^{(2)} \frac{\partial q}{\partial x_2} \left( \frac{\partial \dot{z}_2^{(1)}}{\partial x_1} - \frac{\partial z_2^{(1)}}{\partial x_2} \frac{\partial V_2}{\partial x_1} \right) \\
& + \frac{\partial z_2^{(1)}}{\partial x_1} \frac{\partial q}{\partial x_2} \left( \frac{\partial \sigma_{22}^{(2)}}{\partial x_1} V_1 + \frac{\partial \sigma_{22}^{(2)}}{\partial x_2} V_2 \right) \\
& + \sigma_{22}^{(2)} \frac{\partial z_2^{(1)}}{\partial x_1} \left( \frac{\partial^2 q}{\partial x_1 \partial x_2} V_1 + \frac{\partial^2 q}{\partial x_2^2} V_2 \right) \\
& + \sigma_{22}^{(2)} \frac{\partial z_2^{(1)}}{\partial x_1} \frac{\partial q}{\partial x_2} \frac{\partial V_2}{\partial x_2} \quad (A6)
\end{aligned}$$





$$\begin{aligned}
H_5 = & \sigma_{12}^{(2)} \frac{\partial q}{\partial x_2} \left( \frac{\partial z_1^{(1)}}{\partial x_1} - \frac{\partial z_1^{(1)}}{\partial x_2} \frac{\partial V_2}{\partial x_1} \right) \\
& + \frac{\partial z_1^{(1)}}{\partial x_1} \frac{\partial q}{\partial x_2} \left( \frac{\partial \sigma_{12}^{(2)}}{\partial x_1} V_1 + \frac{\partial \sigma_{12}^{(2)}}{\partial x_2} V_2 \right) \\
& + \sigma_{12}^{(2)} \frac{\partial z_1^{(1)}}{\partial x_1} \left( \frac{\partial^2 q}{\partial x_1 \partial x_2} V_1 + \frac{\partial^2 q}{\partial x_2^2} V_2 \right) \\
& + \sigma_{12}^{(2)} \frac{\partial z_1^{(1)}}{\partial x_1} \frac{\partial q}{\partial x_2} \frac{\partial V_2}{\partial x_2} \quad (A13)
\end{aligned}$$

$$\begin{aligned}
H_6 = & \sigma_{22}^{(2)} \frac{\partial q}{\partial x_2} \left( \frac{\partial z_2^{(1)}}{\partial x_1} - \frac{\partial z_2^{(1)}}{\partial x_2} \frac{\partial V_2}{\partial x_1} \right) \\
& + \frac{\partial z_2^{(1)}}{\partial x_1} \frac{\partial q}{\partial x_2} \left( \frac{\partial \sigma_{22}^{(2)}}{\partial x_1} V_1 + \frac{\partial \sigma_{22}^{(2)}}{\partial x_2} V_2 \right) \\
& + \sigma_{22}^{(2)} \frac{\partial z_2^{(1)}}{\partial x_1} \left( \frac{\partial^2 q}{\partial x_1 \partial x_2} V_1 + \frac{\partial^2 q}{\partial x_2^2} V_2 \right) \\
& + \sigma_{22}^{(2)} \frac{\partial z_2^{(1)}}{\partial x_1} \frac{\partial q}{\partial x_2} \frac{\partial V_2}{\partial x_2} \quad (A14)
\end{aligned}$$

$$\begin{aligned}
H_7 = & \sigma_{12}^{(2)} \frac{\partial q}{\partial x_1} \left( \frac{\partial z_1^{(1)}}{\partial x_2} - \frac{\partial z_1^{(1)}}{\partial x_1} \frac{\partial V_1}{\partial x_2} \right) \\
& + \frac{\partial z_1^{(1)}}{\partial x_2} \frac{\partial q}{\partial x_1} \left( \frac{\partial \sigma_{12}^{(2)}}{\partial x_1} V_1 + \frac{\partial \sigma_{12}^{(2)}}{\partial x_2} V_2 \right) \\
& + \sigma_{12}^{(2)} \frac{\partial z_1^{(1)}}{\partial x_2} \left( \frac{\partial^2 q}{\partial x_1^2} V_1 + \frac{\partial^2 q}{\partial x_1 \partial x_2} V_2 \right) \\
& + \sigma_{12}^{(2)} \frac{\partial z_1^{(1)}}{\partial x_2} \frac{\partial q}{\partial x_1} \frac{\partial V_1}{\partial x_1} \quad (A15)
\end{aligned}$$

$$\begin{aligned}
H_8 = & \sigma_{22}^{(2)} \frac{\partial q}{\partial x_1} \left( \frac{\partial z_2^{(1)}}{\partial x_2} - \frac{\partial z_2^{(1)}}{\partial x_1} \frac{\partial V_1}{\partial x_2} \right) \\
& + \frac{\partial z_2^{(1)}}{\partial x_2} \frac{\partial q}{\partial x_1} \left( \frac{\partial \sigma_{22}^{(2)}}{\partial x_1} V_1 + \frac{\partial \sigma_{22}^{(2)}}{\partial x_2} V_2 \right) \\
& + \sigma_{22}^{(2)} \frac{\partial z_2^{(1)}}{\partial x_2} \left( \frac{\partial^2 q}{\partial x_1^2} V_1 + \frac{\partial^2 q}{\partial x_1 \partial x_2} V_2 \right) \\
& + \sigma_{22}^{(2)} \frac{\partial z_2^{(1)}}{\partial x_2} \frac{\partial q}{\partial x_1} \frac{\partial V_1}{\partial x_1} \quad (A16)
\end{aligned}$$

## References

1. Madsen HO, Krenk S, Lind NC (1986) *Methods of Structural Safety*, Prentice-Hall, Inc., Englewood Cliffs, New Jersey
2. Grigoriu M, Saif MTA, El-Borgi S, Ingraffea A (1990) Mixed-mode fracture initiation and trajectory prediction under random stresses. *Int. J. Frac.* 45: 19–34
3. Provan JW (1987) *Probabilistic Fracture Mechanics and Reliability*, Martinus Nijhoff Publishers, Dordrecht, The Netherlands
4. Besterfield GH, Liu WK, Lawrence MA, Belytschko T (1991) Fatigue crack growth reliability by probabilistic finite elements. *Comp. Meth. Appl. Mech. Eng.* 86: 297–320
5. Besterfield GH, Lawrence MA, Belytschko T (1990) Brittle fracture reliability by probabilistic finite elements. *ASCE J. Eng. Mech.* 116(3): 642–659
6. Rahman S (1995) A stochastic model for elastic-plastic fracture analysis of circumferential through-wall-cracked pipes subject to bending. *Eng. Frac. Mech.* 52(2): 265–288
7. Rahman S, Kim J-S (2000) Probabilistic fracture mechanics for nonlinear structures. Accepted for publication in *Int. J. Pressure Vessels and Piping*
8. Rahman S (2001) Probabilistic fracture mechanics:  $J$ -estimation and finite element methods. *Eng. Frac. Mech.* 68: 107–125
9. Lin SC, Abel J (1988) Variational approach for a new direct-integration form of the virtual crack extension method. *Int. J. Frac.* 38: 217–235
10. deLorenzi HG (1982) On the energy release rate and the  $J$ -integral for 3-D crack configurations. *Int. J. Frac.* 19: 183–193
11. deLorenzi HG (1985) Energy release rate calculations by the finite element method. *Eng. Frac. Mech.* 21: 129–143
12. Haber RB, Koh HM (1985) Explicit expressions for energy release rates using virtual crack extensions. *Int. J. Num. Meth. Eng.* 21: 301–315
13. Barbero EJ, Reddy JN (1990) The Jacobian derivative method for three-dimensional fracture mechanics. *Commun. Appl. Num. Meth.* 6: 507–518
14. Hwang CG, Wawrzynek PA, Tayebi AK, Ingraffea AR (1998) On the virtual crack extension method for calculation of the rates of energy release rate. *Eng. Frac. Mech.* 59: 521–542
15. Feijóo RA, Padra C, Saliba R, Taroco E, Vénere MJ (2000) Shape sensitivity analysis for energy release rate evaluation and its application to the study of three-dimensional cracked bodies. *Comput. Meth. Appl. Mech. Eng.* 188(4): 649–664
16. Haug EJ, Choi KK, Komkov V (1986) *Design Sensitivity Analysis of Structural Systems*, Academic Press, New York, NY
17. Taroco E (2000) Shape sensitivity analysis in linear elastic fracture mechanics. *Comput. Meth. Appl. Mech. Eng.* 188(4): 697–712
18. Chen G, Rahman S, Park YH (2000) Shape sensitivity analysis in linear-elastic fracture mechanics. Submitted to *ASME J. Pressure Vessel Technol*
19. Chen G, Rahman S, Park YH (2000) Shape sensitivity and reliability analyses in linear-elastic fracture mechanics. Submitted to *Int. J. Frac*
20. ABAQUS (1999) *User's Guide and Theoretical Manual*, Version 5.8, Hibbitt, Karlsson, and Sorenson, Inc., Pawtucket, RI
21. Yau JF, Wang SS, Corten HT (1980) A mixed-mode crack analysis of isotropic solids using conservation laws of elasticity. *J. Appl. Mech.* 47: 335–341
22. Moran B, Shih F (1987) Crack tip and associated domain integrals from momentum and energy balance. *Eng. Frac. Mech.* 27: 615–642
23. Nikishkov GP, Atluri SN (1987) Calculation of fracture mechanics parameters for an arbitrary 3-dimensional crack by the equivalent domain integral method. *Int. J. Num. Meth. Eng.* 24: 1801–1821
24. Anderson TL (1995) *Fracture Mechanics – Fundamentals and Applications*, 2nd Edition, CRC Press, Boca Raton, Florida, USA